ABSTRACT

KOTTE, SURENDAR. Investigating the Effect of Sensory Neurons in the Propagation of Tremor. (Under the direction of Dr. Nitin Sharma and Dr. Helen Huang.)

Tremor is a common movement disorder with symptoms characterized by unintentional and uncontrollable rhythmic movements. The tremor manifests in people with Parkinson's disease, essential tremor, and cerebral ataxia, who number more than 11 million in the United States alone. Deep brain stimulation is an effective yet costly tremor suppression treatment that requires surgery. It is recommended only when tremor medications become ineffective. Peripheral afferent nerve stimulation is an alternative non-invasive tremor suppression approach. Recent results with afferent stimulation showed promising results. It is hypothesized that stimulation likely targets peripheral feedback mechanisms that convey muscle spindle feedback to the spinal cord. To test this hypothesis, my thesis investigated the role of sensory neurons in tremor propagation through a computer model of tremor in a wrist. A neuromusculoskeletal model was built to represent wrist movement. This model was then used to investigate the effect of sensory neuron feedback in amplifying induced tremor. An experimental procedure was also established to tune the model characteristics to obtain a fit between experimental and simulated data.

Investigating the Effect of Sensory Neurons in the Propagation of Tremor

by
Surendar Kotte

A thesis submitted to the Graduate Faculty of
North Carolina State University
in partial fulfillment of the
requirements for the Degree of
Master of Science

Electrical Engineering

Raleigh, North Carolina

2021

APPROVED BY:

Dr. Nitin Sharma
Co-chair of Advisory Committee

Dr. Helen Huang
Co-chair of Advisory Committee

Dr. Derek Kamper

BIOGRAPHY

Surendar was born in Tiruvallur a town in Tamil Nadu in India and brought up in Chennai a beautiful coastal city in India. He completed his high school from Velammal School and Secondary education from Maharishi Vidya Mandir in Chennai. He went on to do his Bachelor in Technology degree from National Institute of Technology, Tiruchirapalli majoring in Electronics and Communication Engineering (ECE). He was an active member of the ECE student community and led them to various accolades in the inter department cultural fest. Apart from academics, you can find him playing cricket with his friends or working the with ECE media team.

After graduating, Surendar joined the NC State University to pursue his Master of Science degree majoring in Electrical Engineering specializing in Robotics and Control Systems.

ACKNOWLEDGEMENTS

Firstly, I would like to thank my advisor Dr. Nitin Sharma for his trusting me with this project and supporting me throughout the study. I would like to express my gratitude for the immense patience he showed towards me. His immense knowledge in the field has helped and inspired me to pursue this research.

I would also like to my Co-Chair Dr. Helen Huang and committee member Dr. Derek Kamper for accepting to be a part of my advisory committee.

I would like to extend my gratitude to my fellow lab members Ashwin Iyer, Qiang Zhang and Ziyue Sun for their help with experiments and clearing my doubts whenever I was stuck. Their help was instrumental in completing this thesis.

Lastly, I would like to thank my family and friends for believing in me even when I was not so sure and encouraging me to keep going.

TABLE OF CONTENTS

LIST OF TABLES

LIST OF FIGURES

CHAPTER

1

INTRODUCTION

1.1 Motivation

Tremor is an involuntary, oscillatory and rhythmic movement of a body part [1] and is a very common movement disorder affecting more than 11 million people in the United States alone[2]. Tremor can be caused due to various reasons, the most common being Parkinson's disease, essential tremor, multiple sclerosis [3].

Despite well documented causes and effects of tremors [4],[3], treatment methods are lacking in terms of efficiency and accessibility. The most common methods of treatment are medications and Deep Brain Stimulation (DBS) [5]. Medication are more accessible but are fairly inefficient with only about 50% patients showing significant improvement. DBS has shown more promising efficiency but since it is a surgical procedure, it is recommended only in extreme cases. This makes it a non optimal solution for most situations. DBS has also been shown to have significant side effects.

There are also some specialized devices like weighted pens, tremor resistant cutlery and resistance gloves which solve specific problems that tremor patients might encounter [6]. Although these devices can temporarily alleviate some of the problems, they fail to reliably give an all round solution.

Functional Electrical Stimulation (FES) [7] is another method employed to suppress tremor by using controlled electrical impulses directly on muscles and reduce tremor. But usage of FES even for a short span of time can induce fatigue in the muscles which causes discomfort for the subject and changes the dynamics of muscles and could be painful due to higher current amplitudes.

These drawbacks in the current methods call for a new treatment method. Recent studies suggested that stimulating afferent neurons can be equally effective for tremor suppression instead of efferent fibers. In this study the muscles were stimulated below the threshold of direct muscle activation to avoid stimulation of efferent fibers [8] and target spinal afferent pathways for tremor suppression. This strategy is potentially fatigue resistant and comfortable due to low levels of stimulation intensity. However designing an effective afferent stimulation protocol involves a thorough understanding of the physiology involved in tremor propagation and effect of afferent fibers in tremor amplification.

1.2 Background

Studying tremor involves working with human subjects and performing experiments may be unsafe in the beginning stages. Thus computational modelling can be a useful tool to analyze how different physiological systems interact with each other. Different models have been developed to simulate the different systems in the human body. This greatly simplifies the process of developing a combined model to suit our specific application. [9],[10] used spiking neurons to model the motion at the elbow joint. [11] designed a neural oscillator to model tremor at the elbow and wrist and simulated a functional electrical stimulation to suppress tremor. [12] also studied the recruitment mechanism of motor units and force generation in muscles. Hill muscle model [13] has been extensively used in various studies to model muscle dynamics.

For the current study, the three main systems to be modelled are the neural system, muscular system and the skeletal system. It builds on the study in [14], [1] to build a combined model to model wrist motion and tremor. Physiological data like EMG and IMU [15] is collected through sensors to aid in refining the model parameters and to test the validity of the model. The model developed can be used as a plant to test the control strategies that will be developed. [8],[16],[17].

1.3 Contribution

The aim of this study is to develop a neuromusculoskeletal system to model the movement of wrist and how tremor propagates through peripheral nervous system to the antagonist muscle and is sustained at the wrist joint. Primarily, the role of sensory feedback in tremor amplification is studied. A simple one degree of motion wrist movement is modeled here. Wrist movement and tremor is successfully modelled and the amplification of the tremor due to sensory feedback is documented. Angle data collected using an IMU, and EMG data to measure intent are used to validate the model. The model thus developed will act as a test bed for future tremor characterization and suppression studies.

1.4 Structure of Thesis

The thesis consists of 4 chapters.

Chapter 1 is an introduction to tremor, its causes treatment approaches that motivates the thesis. The background and main contributions are also highlighted.

Chapter 2 presents the neuromusculoskeletal model of the wrist.

In chapter 3, the experimental procedure to record IMU and EMG data is discussed. The data thus obtained will be compared to the simulated data to demonstrate validity of the model.

Chapter 4 summarizes some key insights and proposes future works.

CHAPTER

2

NEUROMUSCULOSKELETAL MODEL

In the human body, brain controls different parts of the body by sending out electrical signals through a system of nerves that connects the brain with all the organs in the human body. The signals generated travel down the spinal cord and reach the organs that are to be controlled. To control the different joints in the human body, the brain sends signals to the muscles attached to the limb. The muscles then generate force which manifests as limb movement [18]. This entire system can be collectively called the neuromusculoskeletal (NMS) system.

In this section, the dynamics and architecture of different parts of the NMS model used to control the wrist joint are discussed. The model consisting of a network of neurons, bi-muscular forearm and skeleton was simulated on SIMULINK (MATLAB, MATHWORKS USA).

2.1 Neuron

Neurons are the basic building blocks of the nervous system [19]. They act as a means of communication between the brain and other parts of the body. Biologically, neurons consist of three basic parts namely dendrite, axon and soma (cell body). Dendrite acts as the input passage, bringing signals from the outside. Axon acts as the output passage which carries signals away from the neurons. The soma acts as a potential accumulator. When the potential inside a neuron exceeds the threshold, discharge occurs which resets the neuron to the resting potential. This event generates a spike which is transmitted out through the axon. Neurons communicate with each other by transmitting spike trains. Neurons that are sending out these spike trains are considered active and neurons that are not transmitting any spikes are considered inactive.

2.1.1 Neuron Behavior

The dynamic behavior of neurons depends on two important factors: recruitment threshold and neuron time constant [12].

2.1.1.1 Recruitment threshold

This is the membrane potential that the neuron has to reach before a spike event occurs. If the threshold is higher, it means the neuron will take longer to activate. If the neuron exceeds the threshold or not depends on the net excitation input. Thus the minimum required input which excites the neuron is called recruitment threshold excitation (RTE).

2.1.1.2 Neuron Time Constant

The rate at which the membrane potential of a neuron increases or decreases is decided by the neuron time constant (τ). If the time constant is high, then the neuron takes longer to charge or discharge and vice versa.

2.2 Neuron Model

The neuron behavior that has been discussed above can be mathematically modelled using a simple differential equation using a leaky integrate and fire formulation and is given by the following equation [20].

$$\dot{V} = -\alpha V + K I \tag{2.1}$$

Here V is the current potential of the neuron and $\dot{V}$ is the rate of change of potential. I is the net afferent signal coming into a particular neuron. α and K are scaling factors which decide the dynamics of a neuron. Different neurons that are modelled will have different afferent signals and scaling factors based on their function and number of signals. $K I$ is the net excitatory drive for a neuron and neuron potential will converge to a value proportional to this. For a neuron to be active, this quantity must be greater than RTE. The factor α is inversely related to the time constant.

Figures 2.1 to 2.3 illustrate the spiking pattern for different excitations. When the excitation is less than RTE, the voltage converges to a value less than the threshold of 1. This does not result in any spiking action. When the excitation is equal to RTE, spiking action starts and spiking action with minimum frequency is observed. When the excitation increases, the frequency of spiking action also increases.

Three different types of neurons are modeled here each having a specific functionality. In the coming subsection, the dynamics, functions, afferent and efferent signals that are being considered for each of the neurons will be detailed.

2.2.1 Motor Neurons

Motor neurons innervate the skeletal muscles and are responsible for the contraction of these muscles [21]. The input signals to these muscles are from three sources namely the cerebral cortex, the sensory neurons , and the interneurons. The output signals from

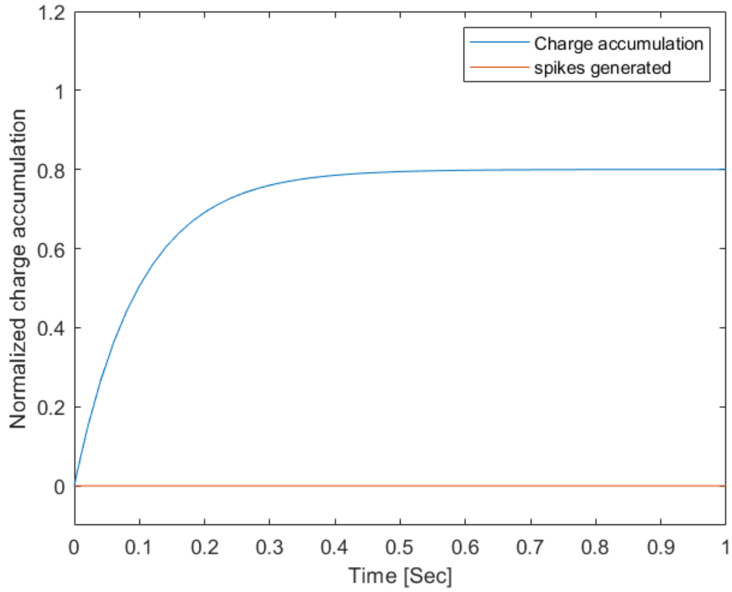

Figure 2.1 Excitation less than RTE

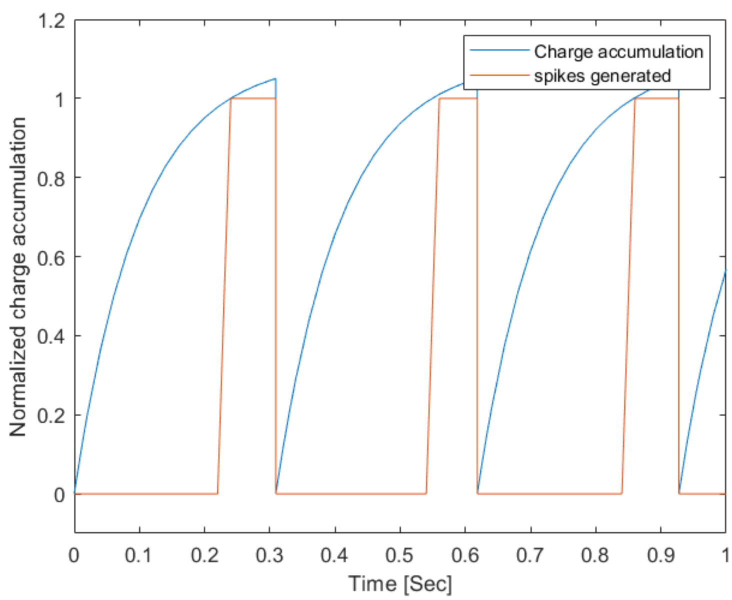

Figure 2.2 Excitation equal to RTE

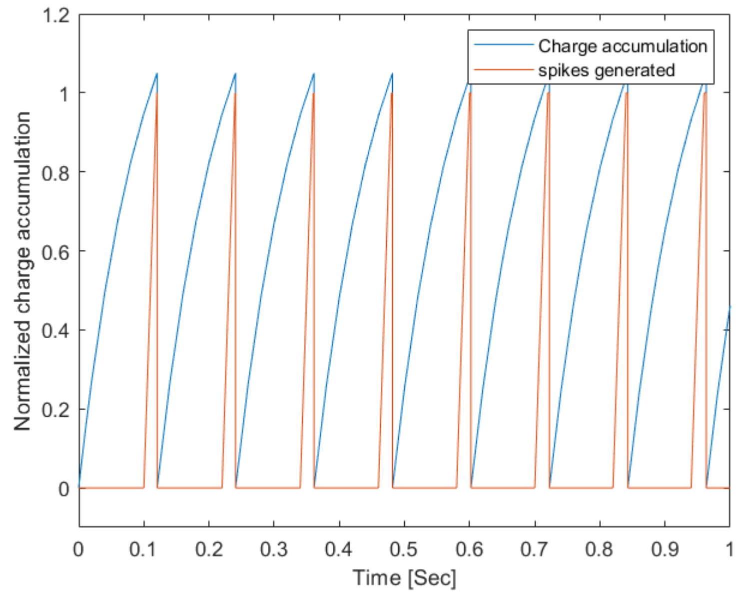

Figure 2.3 Excitation greater than RTE

the motor neurons feed the muscle fibers which contract the muscle. The number of motor neurons in the two muscle system are taken according to the human physiology as $N_{FCR} = 120$ for the flexor carpi radialis (FCR) muscle, which is the agonist muscle and $N_{ECRL} = 120$ for the extensor carpi radialis longus (ECRL) muscle, which is the antagonist muscle. The dynamic behavior of the motor neuron for the agonist and antagonist muscles are obtained by modifying the general LIF equation (2.1) as follows:

$$\dot{X} = -\alpha X + (AS_x - BI_y) + P_x I_f \tag{2.2}$$

$$\dot{Y} = -\beta Y + (CS_y - DI_x) + P_y I_e \tag{2.3}$$

In the above equations, X and Y are the membrane potentials of the agonist and antagonist motor units respectively. α and β are the inverse time constant parameters and A, B, C, D, P_x and P_y are tunable parameters. These parameters can be changed to obtain desirable dynamics of the neurons. The inputs to the FCR in eq. 2.2 are S_x, the sensory feedback from sensory neuron of the flexor, which is an excitatory signal, I_y, the interneuron signal coming from the antagonist muscle which is an inhibitory signal, and I_f, the intent signal from the brain. The values of the parameters used in the model are given in table 2.1. Similarly in eq. 2.3, S_y, I_x and I_e are the excitatory sensor feedback, inhibitory interneuron signal and intent signal from the brain.

Table 2.1 Motor Neurons model parameters

α, β	A, B, C, D	P_x, P_y
1	1	50

2.2.2 Muscle spindle

Muscle spindles are stretch receptors which detect the change in length and the velocity of muscles [22]. This information is conveyed back to the brain via the Ia sensory fibers. The brain then uses this information and estimates the current limb position. This process is called proprioception. It is also used to regulate the contraction of the muscles. The length and velocity of the muscle is coded as a signal which is given by the power law [9]. The muscle spindle output feeds the motor neuron and the interneurons.

$$s(t) = 4.3v(t)^{0.6} + 2l(t) + 10 \tag{2.4}$$

$s(t)$ is the coded sensory signal for each muscle spindle. $l(t)$ and $v(t)$ are the residual length and velocity of the muscle respectively. The residual length is the difference between the current length and the resting length of the muscle. The number of muscle spindle is taken as 50 for FCR and 100 ECRL. In this study, the length and velocity of the muscle is estimated using the angle and angular velocity of the wrist. The formula for estimation is discussed in a later section.

2.2.3 Interneurons

Interneurons connect the sensory neurons to the motor neurons. This kind of connection is called a di-synaptic connection. This signal acts as an inhibitory signal to the opposite muscle. Under flexion, ECRL is inhibited and under extension, FCR is inhibited. To model the interneurons, we again modify the LIF formulation eq.2.1 as follows

$$\dot{I}_x = -\gamma_x I_x + E_x S_x \tag{2.5}$$

$$\dot{I}_y = -\gamma_y I_y + E_y S_y \tag{2.6}$$

Here I refers to the membrane potential and $\dot{I}$ refers to the change in membrane potential. S refers to the afferent signals from muscle spindle. γ and E refer to tunable parameters to obtain desirable dynamics. Subscripts x and y refer to the agonist and antagonist muscle respectively. The number of interneurons is taken as 50 for FCR and 100 for ECRL. The values of the parameters used to model the interneurons are given in table 2.2.

Table 2.2 Interneurons model parameters

γ_x, γ_y	E_x, E_y
1	1

2.3 Muscular Model

To control the wrist, a two muscle model is used. When a muscle receives a signal, it gets activated and starts contracting. When there is no activation, it expands to its optimal length unless held in place by an antagonist muscle. There is no mechanism to control the expansion of a muscle. Thus to enable flexion and extension, two muscles are needed which work out of phase with each other. In the two muscle system, two control signals one for each muscle is produced. This control signal is in the form of spikes as discussed in the previous sections. Muscles in our body convert spike events into twitch forces. Summation of these twitch forces results in the instantaneous muscle force [12]. The force generation can be decomposed into two steps:

2.3.1 Muscle Activation

The incoming spikes from motor neurons activate the muscles and this is modelled as an impulse response to a second order system [11] given as

$$a_i(t) = \frac{t}{T_i} e^{1-\frac{t}{T_i}} \tag{2.7}$$

Here T_i refers to the time to reach the peak activation of the i^{th} motor unit respectively. T_i is taken as a constant value for all neurons in this study.

Fig.2.4 illustrates the impulse response of muscle activation. The activation reaches a maximum value of 1 in time T = 40ms and then goes to zero.

2.4 Activation to Force

An activated muscle produces a twitch force and this force depends on multiple factors. Activation to twitch force is computed using the Hill model equation [13]. The different components of the Hill Model are discussed next.

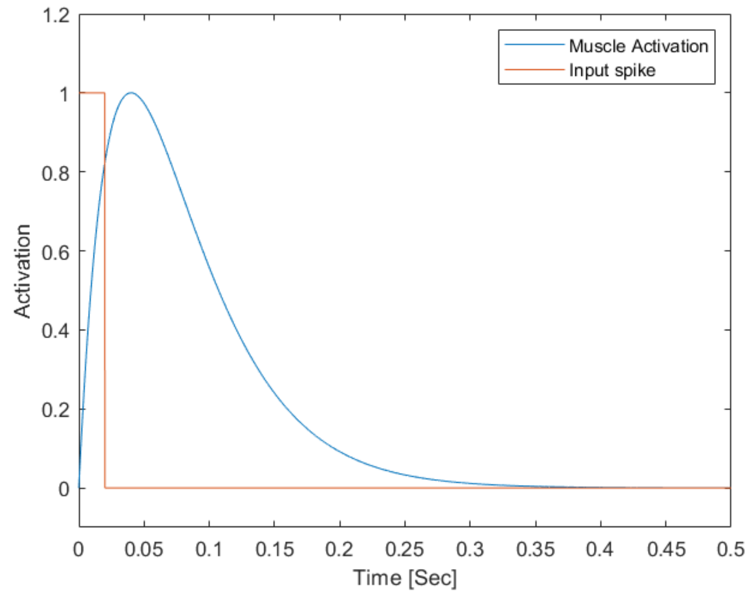

Figure 2.4 Muscle activation as an impulse response

2.4.1 Length Factor

The instantaneous length of the muscle affects the force output of the muscle. The closer the length is to the optimal length, higher is the force produced. A Gaussian like function is used to model this behavior [1].

$$f_l = exp[-(\frac{\bar{l}-1}{\varepsilon})^2] \tag{2.8}$$

Here ε is a tunable parameter and $\bar{l}$ is the normalized length of the muscle given as

$$\bar{l} = \frac{l}{l_{opt}} \tag{2.9}$$

where l_{opt} is the optimum length of the muscle and l is estimated as

$$l = r(\theta - \theta_0) \tag{2.10}$$

where θ_0 is the resting angle of the arm and is taken as 0 for the simulation and r is the moment arm given in Table 2.4.

Fig. 2.5 illustrates the relation between muscle length and force length factor. f_l is maximum

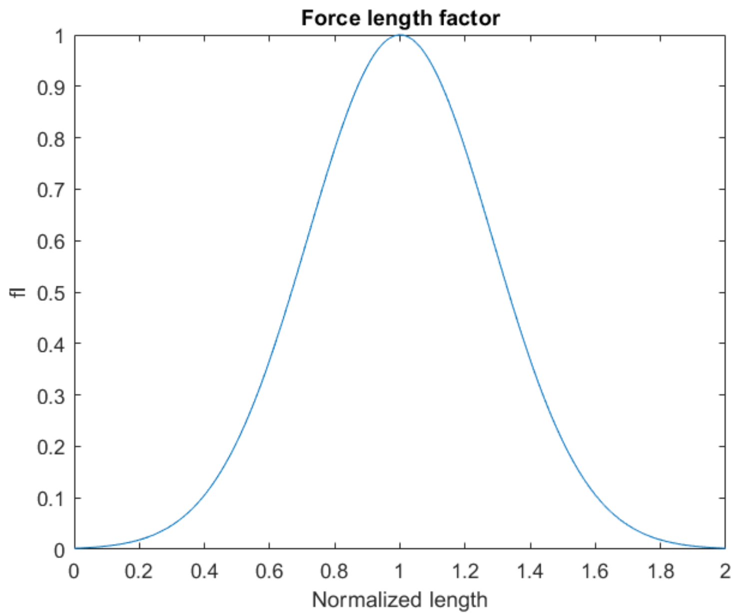

Figure 2.5 Illustration of force length factor

when the normalized length is 1 which means the muscle is at the optimum length. As the length of the muscle varies around the optimum length, f_l decreases and thus the force output also decreases.

2.4.2 Velocity Factor

The velocity of contraction also affects the force output. A hyperbola like function [1] can capture this behavior and the relation is given as follows.

$$f_v = 0.54 tan^{-1}(5.69\bar{v} + 0.51) + 0.745 \tag{2.11}$$

where $\bar{v}$ is the normalized velocity given as

$$\bar{v} = \frac{v}{v_{max}} \tag{2.12}$$

where v_{max} is the maximum achievable velocity of the muscle and v is estimated as

$$l = r\dot{\theta} \tag{2.13}$$

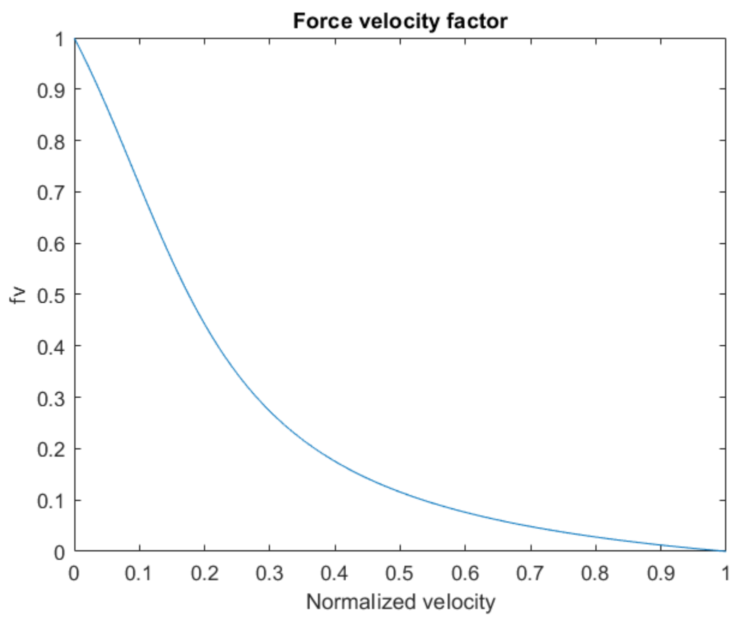

Figure 2.6 Illustration of force velocity factor

Fig.2.6 illustrates the relation between the muscle velocity and force output. It can be seen that when the muscle velocity is zero, f_v is 1 but as it starts contracting, f_v decreases thus force output also decreases. When the velocity reaches the maximum value, the force output becomes zero. This ensures that the muscle does not accelerate any more.

2.4.3 Hill Model

Hill model combines the activation (2.7), length factor (2.8) and velocity factor (2.11) along with peak force P_i for motor unit i as follows [13]:

$$f_i(t) = P_i a_i(t) f_l f_v \tag{2.14}$$

The total force generated by a muscle is the summation of twitch forces from all motor units.

$$F(t) = \sum_{i=1}^{N} f_i(t) \tag{2.15}$$

where N is the number of motor units.

The initial values taken for the different model parameters are given in the Table

Table 2.3 Muscular model parameters

Muscle	T	l_{opt}	v_{max}	P_i
FCR	40ms	0.051	0.255	2
ECRL	40ms	0.081	0.405	2

2.4.4 Muscle Passive Torque

Passive torque is the resistance offered by the muscle to movement even when the muscle is not active [11]. It acts to oppose the movement. It is given as follows

$$T_p = k_0\theta + b_0\dot{\theta} + k_2(e^{k_1\theta} - 1) \tag{2.16}$$

where θ is the current wrist joint angle and $\dot{\theta}$ is the angular velocity of the wrist. k_0, k_1, k_2, b_0 are constant coefficients found to match the experimental data and are -1.6 Nm/rad, -

1.3/rad, 0.5 Nm, and -1.2 Nm/rad respectively.

2.5 Skeleton Model

The wrist skeleton is modelled as 1 DOF damped oscillator [11]. The angular velocity of the wrist is given as

$$\ddot{\theta} = [(F_1 r_1 - F_2 r_2) + T_p]/I \tag{2.17}$$

Here F_1, F_2 are forces from FCR and ECRL muscles and r_1 and r_2 are the moment arms. I is the moment of inertia of the wrist. T_p is the passive torque from eq. 2.16. The values used are given in the Table 2.4

Table 2.4 Muscular model parameters

Mass m	Length l	Moment arm r_1	Moment arm r_2
0.43	0.18	0.019	0.018

2.6 Architecture

The various modules discussed in this section are interconnected as shown in fig.2.7. A command is given as the input to the Neural Network along with signals from the sensor networks. The spike train thus generated from the neurons is fed to the muscular model which produces muscle activation and the force. The force generated is fed to the skeleton and this is exhibited as the output angle. Length and velocity of the muscles is then fed to the sensor networks which modulate them as a sensor signal which is fed back to the neural network.

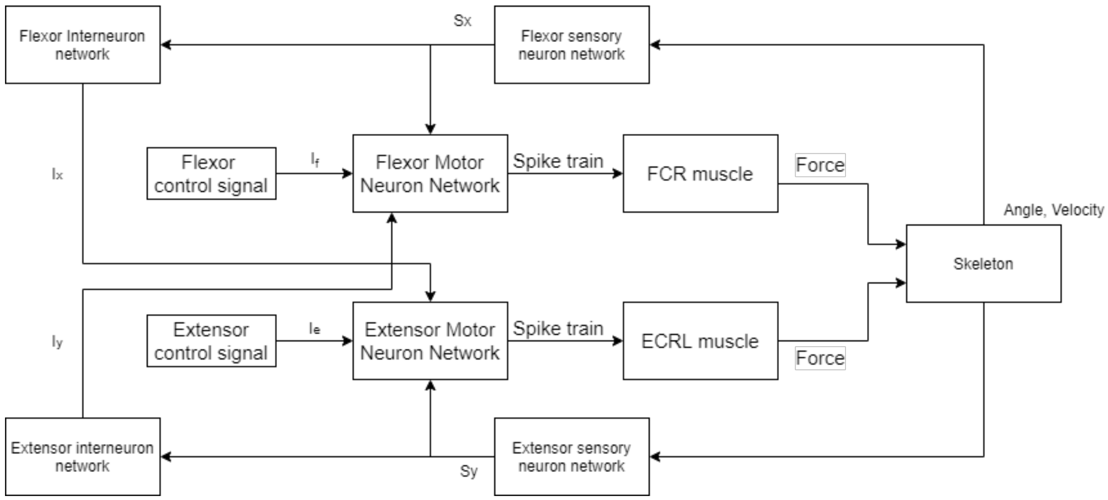

Figure 2.7 Architecture of model

2.7 Simulation results

The model developed in this section was used to simulate the wrist flexion. Tremor is induced as a noisy intent and the wrist angle is plotted. A power spectrum performed on the angle is then used to study the effect of the sensory neurons in the tremor transmission. The power spectrum gives the estimate of how much energy is contained at each frequency in a signal. Fourier transform of a discrete signal $x(n)$ is given as follows

$$X(k) = \sum_{n=0}^{N-1} x(n) e^{-\frac{i2\pi}{N}kn} \tag{2.18}$$

Using eq. 2.18, the log power spectrum [23] can be estimated as

$$S(f) = 2log_{10}(|X(f)|) \tag{2.19}$$

2.7.1 Wrist flexion

To model flexion, a higher movement intent was given to the FCR motor neurons and a lower intent to the ECRL motor neurons. This results in a movement towards the positive direction.

2.7.1.1 No Tremor Induced.

Fig. 2.8 illustrates the wrist movement when there is no tremor for two scenarios when the sensory feedback is turned on and when it is turned off. The baseline signal is when the feedback is turned off. When the feedback is turned on, we can observe two things. The trajectory is affected. This is a combination of two factors the excitatory sensory feedback and inhibitory interneuron feedback. The combined effect pulls the angle down. The second observation is that there is some oscillation introduced in the angle. This is primarily due to unoptimized system parameters. By performing Fourier analysis, we can see that the oscillation introduced does not fall in any particular frequency range but is introduced uniformly across the entire spectrum. This can be seen in fig. 2.9. A zoomed image in fig. 2.10 shows the frequency range of tremor around 3 to 5 Hz and we can observe that there is no significant spike at any frequency indicating that the oscillations do not belong to a particular frequency.

2.7.1.2 Monotonic tremor induced

A 3Hz sine component was added to the intent to simulate tremor and this manifests as a 3Hz oscillation in the angle which is illustrated in fig. 2.11. The same two observations can be seen but additionally both with and without sensory feedback, a periodic 3Hz oscillation can be seen. This is the tremor oscillation. But more importantly, the oscillation intensity is higher when feedback is turned on. It can be further illustrated in fig. 2.13 where there are spikes at 3Hz. But the spike when feedback is turned on is much more prominent than when the feedback is turned off.

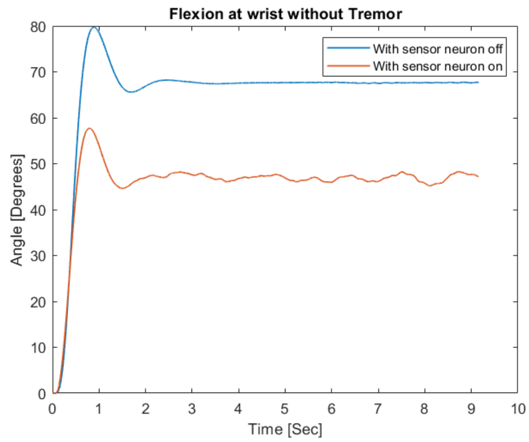

Figure 2.8 Wrist flexion without tremor

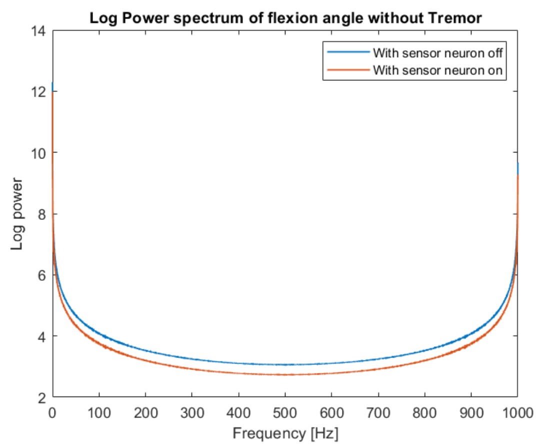

Figure 2.9 Power Spectrum of wrist angle without tremor

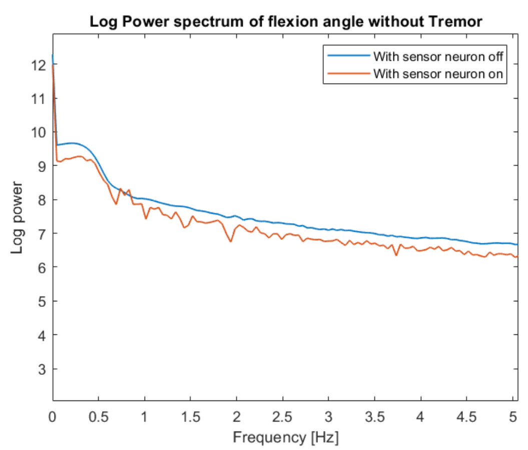

Figure 2.10 Zoomed Power Spectrum of wrist angle without tremor

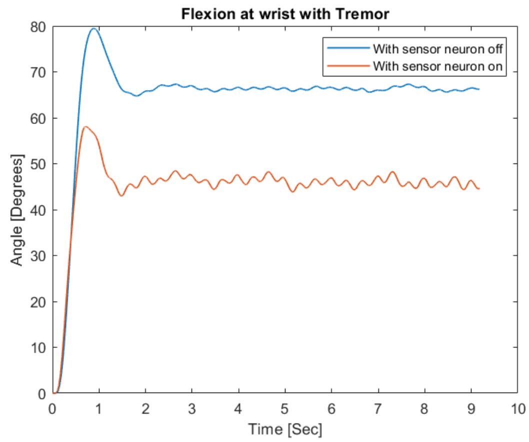

Figure 2.11 Wrist flexion with tremor

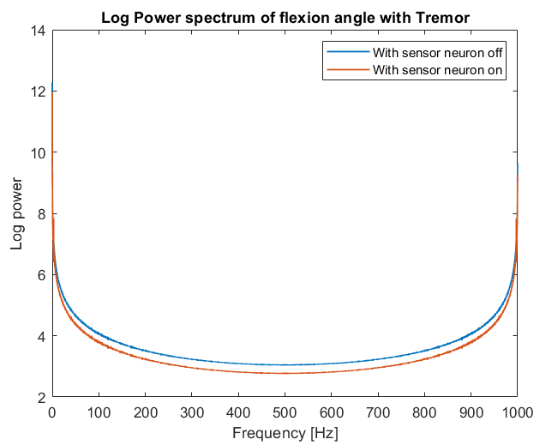

Figure 2.12 Power Spectrum of wrist angle with tremor

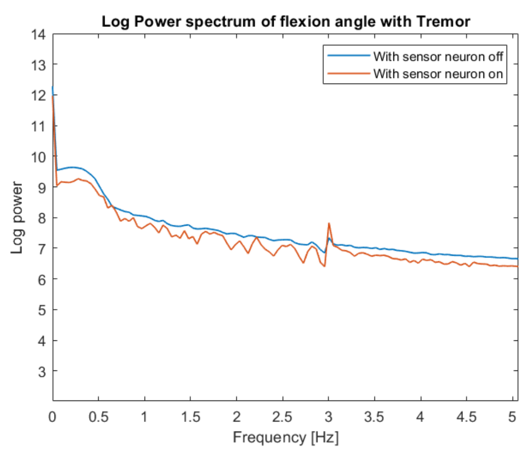

Figure 2.13 Zoomed Power Spectrum of wrist angle with tremor

2.8 Discussion

From Fig. 2.8 to Fig. 2.13, we have established that the trajectory of the wrist and tremor intensity is heavily influenced by sensory feedback. Introducing sensory feedback mechanism amplifies the induced tremor. This is the key insight we are looking to obtain from this study. This leads us to fact that muscle spindle feedback contribute to the oscillations induced at the wrist joint. Traditional FES systems use electrical impulses to stimulate the muscles directly. This often leads to muscle fatigue. Instead using the insight from the simulation results, one can design an alternative treatment that stimulates the sensory neurons and altering the feedback that is travelling up the spinal cord, provides a fatigue resistant and a comfortable non-invasive stimulation treatment for tremor.

CHAPTER

3

EXPERIMENTS

In this section, results from model validation experiments are presented and the data acquisition and processing steps are discussed. Preliminary test was conducted on one male participant aged 24 with no disability. Approval for the experiment was obtained from the NCSU Institutional Review Board (IRB protocol number : 19247).

3.1 Experimental Procedure

The experiment was designed to acquire electromyogram data from muscles and wrist angle data. The subject was seated and the sensors were strapped on his right forearm. The subject was then asked to perform flexion and extension at a low frequency till an angle of about 60°. The trial was repeated six times and the best noise free data obtained was stored for processing. Simulink models were written for data acquisition for each of the sensors and run on external hardware. Fig3.1 illustrates the experimental setup showing the strapped sensors on the subject's hand and forearm.

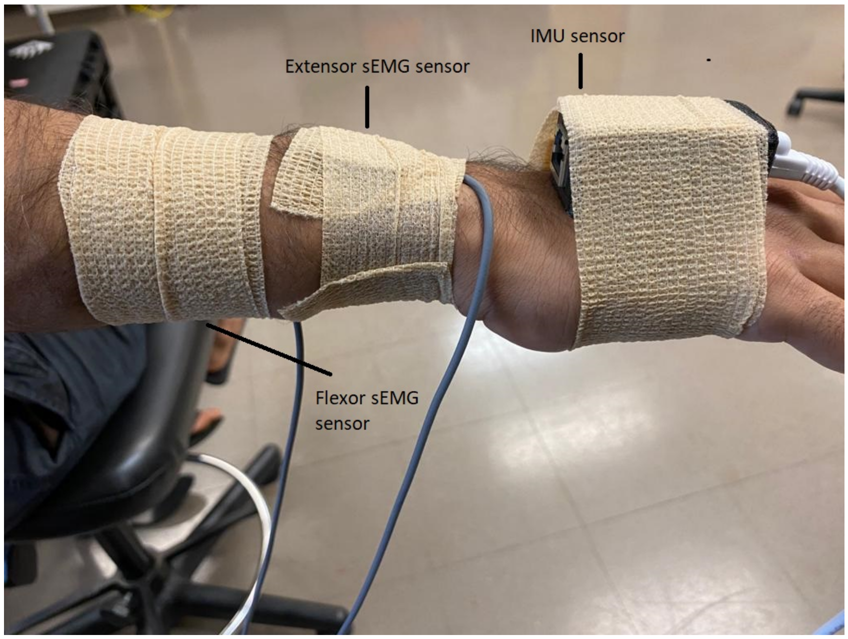

Figure 3.1 Experimental Setup

3.2 Electromyogram signal

Electromyogram (EMG) gives information about muscle activation and in turn the intent at that particular muscle. If the muscle is activated, there is a spike in the activation. This is reflected in the EMG. Thus by measuring the EMG signals at the flexor and extensor at the wrist, we can estimate the intent to move the muscle. Here the surface EMG (sEMG) signals were recorded.

3.2.1 Data Acquisition

sEMG sensors were placed on the flexor and the extensor which are about 5cm from the rotation centers of the wrist joint and reference electrode was placed on the belly. The electrodes were connected to BagnoliTM Desktop (DELSYS, MA, USA) which was connected to speedgoat to input data into the desktop [24]. Data was collected at a sampling rate of 1KHz and was stored for offline processing.

3.2.2 Data Processing

The obtained data was processed on MATLAB. An averaging kernel was convolved with the obtained signal and normalized to limit between 0 and 1. The signal was further down-sampled to obtain a final sampling frequency of 10Hz. Fig. 3.2 to fig. 3.3 show the different stages in EMG data processing.

3.3 Inertial Measurement Unit

The Inertial Measurement Unit (IMU) is used to record the current state of the wrist. An IMU sensor generates signal proportional to the current roll, pitch and yaw of the sensor. This raw signal can be processed to obtain the current angle in the xyz space.

3.3.1 Data Acquisition

IMU sensor was strapped to the top of the hand and the sensor was connected to a Raspberry Pi which collected the raw signal and transferred them to the PC over an ethernet cable. The data was sampled at a sampling rate of 1KHz.

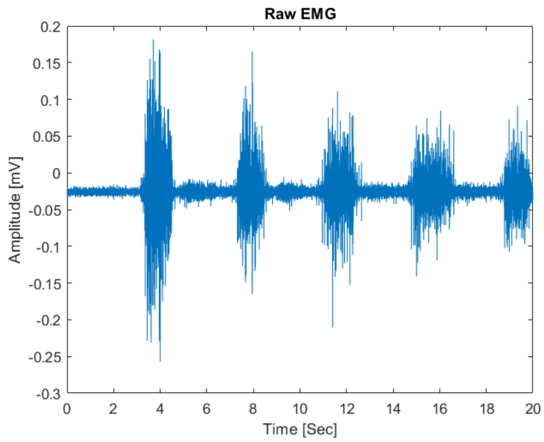

Figure 3.2 Raw EMG data from sensor

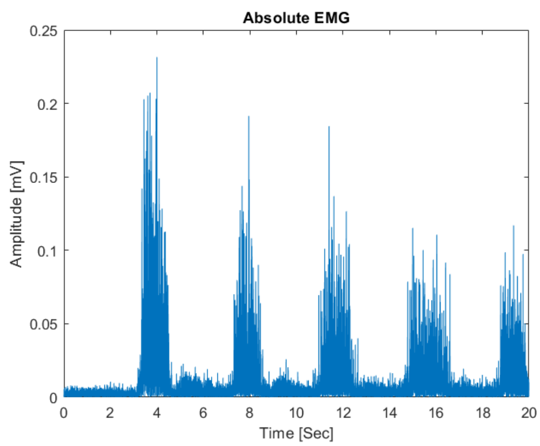

Figure 3.3 Absolute value of EMG

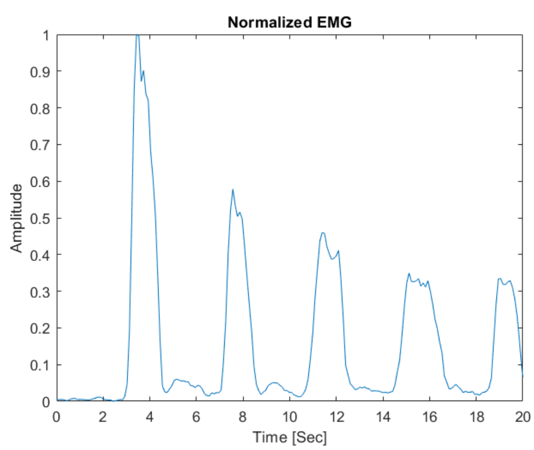

Figure 3.4 Filtered and normalized EMG data

3.3.2 Data Processing

To process the IMU signal, the raw readings were passed through a first order complimentary filter. The readings were then converted to radians and down-sampled to match the rate of EMG readings. Fig. 3.5 shows the processed IMU data.

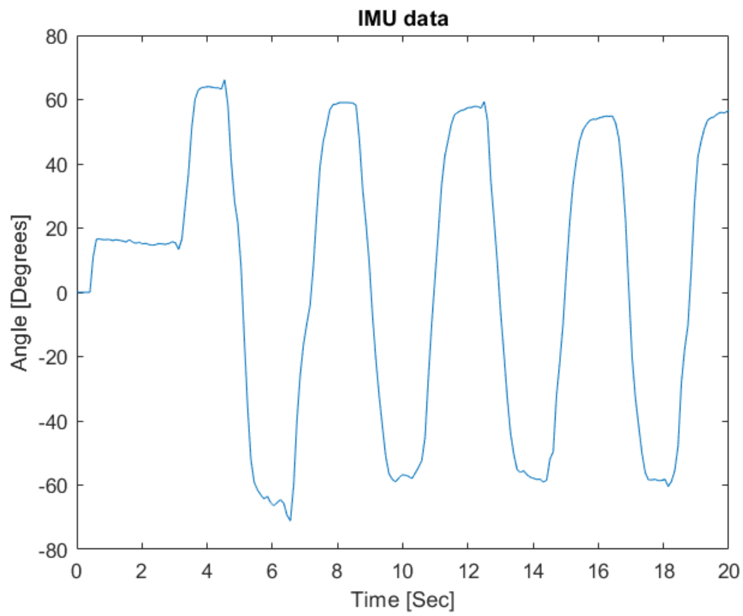

Figure 3.5 Sample IMU data

3.4 Model tuning and validation

The processed sEMG was given as the intent input to the motor neurons and the output angle was recorded. Model parameters were manually tuned to obtain a wrist angle which closely resembled the measured angle from the IMU. Once a tuned model was obtained, the second trial was used for validation. The fit for the validation dataset is shown in fig. 3.6.

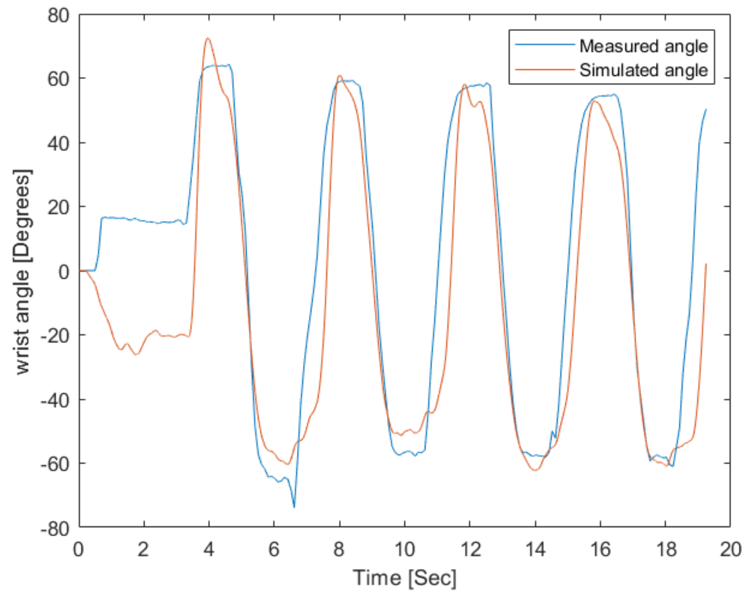

Figure 3.6 Validation fit on experimental data

3.5 Discussion

Data collected from the experiment can be used to calibrate the model parameters and subject specific model can be obtained. This is an important step in tremor modelling since different subjects' wrist will react differently to stimulation. The process can be automated by using system identification techniques [9].

CHAPTER

4

CONCLUSION

The aim of the study had two objectives. 1. To build a Neuromusculoskeletal model to represent a wrist joint capable of flexion and extension and simulate tremor induction. 2. To study the effect of sensory neurons in sustaining and amplifying tremor once it is induced. Through the developed computational model, we can draw preliminary observations that potentially point out the role of sensory feedback during the tremor propagation.

4.1 Preliminary Insights

The simulations point out to some extent that the sensory feedback that goes into the motor neurons is a factor in the tremor amplification. This was illustrated Fourier analysis that showed increase in the power of tremor frequency when the sensory feedback is involved.

Preliminary experiments also suggest that the proposed model predicts movement, when EMG is used as a surrogate for the descending signals. Thus the model may be used in the tremor studies.

4.2 Future work

4.2.1 Model Optimization

Although manual tuning of some system parameters gave a good fit for the experimental data, an optimization paradigm to find model parameters is needed to fit measured angle with the simulated angle. Thus work needs to be done in this direction to obtain a data driven model that can be generalized to different tremor frequency and limbs.

4.2.2 Ultrasound imaging

The muscle length and velocity in the experiment were estimated using the wrist angle and the angular velocity. Instead ultrasound imaging [24] can be directly used to estimate the muscle length and velocity. Direct measurements from ultrasound imaging can potentially avoid introduction of unwanted uncertainties during limb angle to muscle length transformation.

4.2.3 Control system development

Once a data driven tremor model is obtained, a control system to suppress tremor can be developed. An integrator back-stepping based controller [25] to account for cascaded motor unit and sensory feedback dynamics can be developed. This will help subject suffering from essential tremor and Parkinson's disease in performing day to day activities without hindrance from the tremor.

BIBLIOGRAPHY

[1] Zhang, Z. et al. "Modeling and Identification of Electrically Stimulated Muscles for Wrist Movement". *2018 15th International Conference on Control, Automation, Robotics and Vision (ICARCV)*. 2018, pp. 1823–1828.

[2] Louis, E. D. & Ferreira, J. J. "How common is the most common adult movement disorder? Update on the worldwide prevalence of essential tremor". *Movement disorders : official journal of the Movement Disorder Society* **25**.5 (2010), 534—541.

[3] Helmich, R. C. et al. "Cerebral causes and consequences of parkinsonian resting tremor: a tale of two circuits?" *Brain* **135**.11 (2012), pp. 3206–3226. eprint: `https://academic.oup.com/brain/article-pdf/135/11/3206/753076/aws023.pdf`.

[4] Louis, E. D. "Non-motor symptoms in essential tremor: A review of the current data and state of the field". *Parkinsonism Related Disorders* **22** (2016). Proceedings of XXI World Congress on Parkinson's Disease and Related Disorders, December 6-9, 2015, Milan, Italy, S115–S118.

[5] Deuschl, G. et al. "Treatment of patients with essential tremor". *The Lancet Neurology* **10**.2 (2011), pp. 148–161.

[6] Mo, J. & Priefer, R. "Medical Devices for Tremor Suppression: Current Status and Future Directions". *Biosensors* **11**.4 (2021).

[7] Prochazka, A. et al. "Attenuation of pathological tremors by functional electrical stimulation I: Method". *Annals of Biomedical Engineering* (1992), pp. 205–224.

[8] Barroso, F. et al. "Review on Tremor Suppression Using Afferent Electrical Stimulation". English (US). *Biosystems and Biorobotics*. Biosystems and Biorobotics. Springer International Publishing, 2019, pp. 1092–1096.

[9] Sreenivasa, M. et al. "Modeling and Identification of a Realistic Spiking Neural Network and Musculoskeletal Model of the Human Arm, and an Application to the Stretch Reflex". *IEEE Transactions on Neural Systems and Rehabilitation Engineering* **24**.5 (2016), pp. 591–602.

[10] Sreenivasa, M. et al. "Modeling and identification of the human arm stretch reflex using a realistic spiking neural network and musculoskeletal model". *2013 IEEE/RSJ International Conference on Intelligent Robots and Systems*. 2013, pp. 329–334.

[11] Zhang, D. et al. "Neural oscillator based control for pathological tremor suppression via functional electrical stimulation". *Control Engineering Practice* **19**.1 (2011), pp. 74–88.

[12] Fuglevand, A. et al. “Fuglevand, A. J., Winter, D. A. Patla, A. E. Models of recruitment and rate coding organization in motor-unit pools. J. Neurophysiol. 70, 2470-2488”. *Journal of neurophysiology* **70** (1993), pp. 2470–88.

[13] Winters, J. M. “Hill-Based Muscle Models: A Systems Engineering Perspective”. *Multiple Muscle Systems: Biomechanics and Movement Organization*. Ed. by Winters, J. M. & Woo, S. L.-Y. New York, NY: Springer New York, 1990, pp. 69–93.

[14] Yao, P. et al. “Simulation of Tremor on 3-Dimentional Musculoskeletal Model of Wrist Joint and Experimental Verification”. *Conference proceedings : ... Annual International Conference of the IEEE Engineering in Medicine and Biology Society. IEEE Engineering in Medicine and Biology Society. Conference* **2012** (2012), pp. 4823–6.

[15] Dideriksen, J. L. et al. “A Model of the Surface Electromyogram in Pathological Tremor”. *IEEE Transactions on Biomedical Engineering* **58**.8 (2011), pp. 2178–2185.

[16] Copur, E. H. et al. “Repetitive Control of Electrical Stimulation for Tremor Suppression”. *IEEE Transactions on Control Systems Technology* **27**.2 (2019), pp. 540–552.

[17] Manto, M. et al. “Dynamically responsive intervention for tremor suppression”. *IEEE Engineering in Medicine and Biology Magazine* **22**.3 (2003), pp. 120–132.

[18] Yeom, H. G. et al. “Brain mechanisms in motor control during reaching movements: Transition of functional connectivity according to movement states”. *Scientific Reports* **10** (2020).

[19] Bullock, T. H. et al. “The Neuron Doctrine, Redux”. *Science* **310**.5749 (2005), pp. 791–793. eprint: `https://science.sciencemag.org/content/310/5749/791.full.pdf`.

[20] Lansky, P. et al. “The parameters of the stochastic leaky integrate-and-fire neuronal model”. **21** (2006), pp. 211–223.

[21] Stifani, N. “Motor neurons and the generation of spinal motor neurons diversity”. *Frontiers in Cellular Neuroscience* **8** (2014), p. 293.

[22] Hulliger, M. “The mammalian muscle spindle and its central control”. *Reviews of Physiology, Biochemistry and Pharmacology, Volume 101: Volume: 101*. Berlin, Heidelberg: Springer Berlin Heidelberg, 1984, pp. 1–110.

[23] “Chapter 3 Power spectrum and its applications”. *Analysis of Geophysical Potential Fields*. Ed. by Naidu, P. S. & Mathew, M. Vol. 5. Advances in Exploration Geophysics. Elsevier, 1998, pp. 75–143.

[24] Iyer, A. et al. “Analysis of Tremor During Grasp Using Ultrasound Imaging: Preliminary Study”. *2020 8th IEEE RAS/EMBS International Conference for Biomedical Robotics and Biomechatronics (BioRob)*. 2020, pp. 533–538.

[25] Alibeji, N. et al. “Dynamic surface control of neuromuscular electrical stimulation of a musculoskeletal system with activation dynamics and an input delay”. *2015 American Control Conference (ACC)*. 2015, pp. 631–636.

APPENDIX

APPENDIX

A

SIMULINK MODEL OF NEUROMUSCULOSKELETAL MODEL

A.1 Modelling

The NMS model was built and simulated on simulink. The different aspects like introducing intention, tremor will be discussed here. Fig. A.1 illustrates the block diagram of the NMS model. If and Ie are the input signals which drive the wrist.

A.1.1 Modelling Neuron

To model the neuron, the dynamics equation eq. 2.2 and 2.3 are solved using a user defined function. An integrator is then used to get X and Y from $\dot{X}$ and $\dot{Y}$. The integrator is wrapped

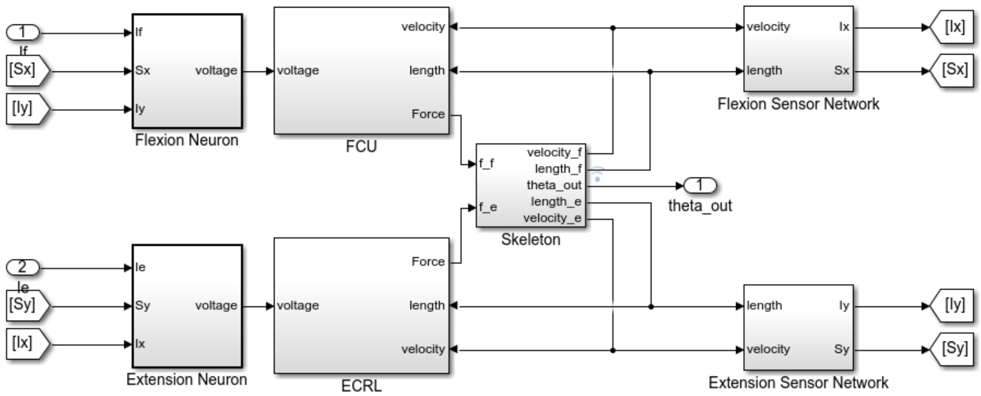

Figure A.1 Simulink model of NMS

when the value reaches the threshold of 1. This ensures that the value resets to 0. A switch block is then used to convert voltage into spike trains. The same structure was used for Motor neuron and Interneuron. Fig. A.2 illustrates this structure.

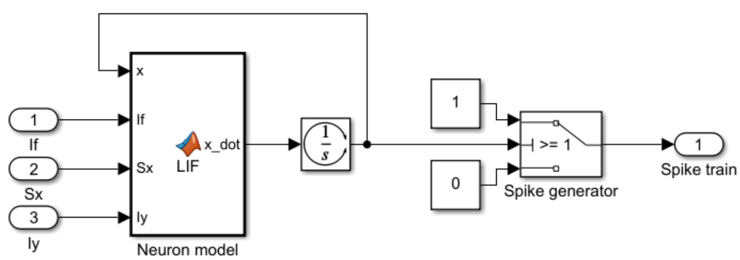

Figure A.2 Simulink model of Neuron

A.1.2 Modelling muscle

In a muscle, every spike should induce a single response. This entails that every spike should reset the clock associated with its muscle spindle. This is accomplished by using a clock generator. The clock generated is then given as input to the hill model along with the estimate of length and velocity of the muscle. The force thus generated is filtered to remove noise. The model used is given in fig. A.3.

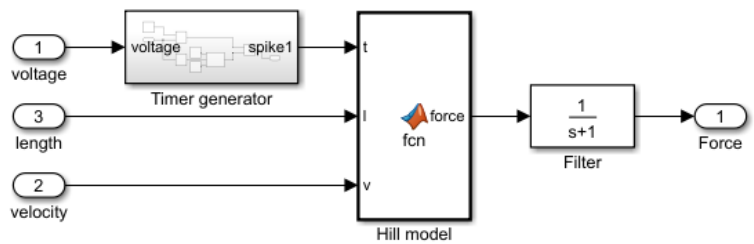

Figure A.3 Simulink model of Muscle

A.1.3 Modelling wrist intent

To model wrist movement, input signals I_e and I_f is generated as a sine wave. The general form of a sine wave is $A + Bsin(\omega t + \phi)$ where A is the bias, B is the gain, ω is the frequency in radians/s and ϕ is the phase shift in radians. For the wrist, A is the intention and the term B$sin(\omega t + \phi)$ is the tremor signal. To induce tremor of different frequencies and intensities, ω and B can be altered. The signals are made out of phase by setting the phase ϕ for flexion and extension as 0 and π respectively.

To turn the sensor feedback on and off a gain block has been introduced between the lines. To turn the line on, gain is set to 1 and to turn it off, the gain is set to 0.